Contrasting responses of phytoplankton productivity between coastal and offshore surface waters in the Taiwan Strait and the South China Sea to short-term seawater acidification

Guang Gao[1], Tifeng Wang[1], Jiazhen Sun[1], Xin Zhao[1], Lifang Wang[1], Xianghui Guo[1], Kunshan Gao[1,2]*

[1]State Key Laboratory of Marine Environmental Science & College of Ocean and Earth Sciences, Xiamen University, Xiamen 361005, China

[2]Co-Innovation Center of Jiangsu Marine Bio-industry Technology, Jiangsu Ocean University, Lianyungang 222005, China

*Corresponding author: ksgao@xmu.edu.cn

Abstract

Seawater acidification (SA) has been documented to either inhibit or enhance or result in no effect on marine primary productivity (PP). In order to examine effects of SA in changing environments, we investigated the influences of SA (a decrease of 0.4 pH_{total} units with corresponding CO_2 concentrations ranged 22.0–39.7 μM) on PP through deck-incubation experiments at 101 stations in the Taiwan Strait and the South China Sea, including the continental shelf and slope, as well as deep-water basin. The daily primary productivities in surface seawater under incident solar radiation ranged from 17–306 μg C (μg Chl *a*)$^{-1}$ d^{-1}, with the responses of PP to SA being region-dependent and the SA-induced changes varying from -88% (inhibition) to 57% (enhancement). The SA-treatment stimulated PP in surface waters of coastal, estuarine and shelf waters, but suppressed it in the South China Sea basin. Such SA-induced changes in PP were significantly related to in situ pH and solar radiation in surface seawater, but negatively related to salinity changes. Our results indicate that phytoplankton cells are more vulnerable to a pH drop in oligotrophic waters. Contrasting responses of phytoplankton productivity in different areas suggest that SA impacts on marine primary productivity are region-dependent and regulated by local environments.

Keywords: CO_2; Taiwan Strait; seawater acidification; photosynthesis; primary productivity; South China Sea

1 Introduction

The oceans have absorbed about one-third of anthropogenically released CO_2, which increased dissolved CO_2 and decreased pH of seawater (Gattuso et al., 2015), leading to ocean acidification (OA). This process is ongoing and likely intensifying (IPCC, 2019). OA has been shown to result in profound influences on marine ecosystems (see the reviews and literature therein, Mostofa et al., 2016; Doney et al., 2020). Marine photosynthetic organisms, which contribute about half of the global primary production, are also being affected by OA (see the reviews and literatures therein, Riebesell et al., 2018; Gao et al., 2019a). In addition to the slow change of ocean acidification, some processes, such as freshwater inputs, upwelling, typhoon and eddies, can lead to instantaneous CO_2 rising and short-term changes in carbonate chemistry, termed seawater acidification (SA) (Moreau et al., 2017; Yu et al., 2020). Since SA occurs in many locations of ocean, it is important to understand the responses of the key players of marine biological CO_2 pump, the phytoplankton, to seawater acidification.

Elevated CO_2 is well recognized to lessen the dependence of algae and cyanobacteria on energy-consuming CO_2 concentrating mechanisms (CCMs) which concentrate CO_2 around Rubisco, the key site for photosynthetic carbon fixation (Raven & Beardall, 2014 and references therein; Hennon et al., 2015). The energy freed up from the down-regulated CCMs under increased CO_2 concentrations can be applied to other metabolic processes, resulting in a modest increase in algal growth (Wu et al., 2010; Hopkinson et al., 2011; Xu et al., 2017). Accordingly, elevated CO_2 availability could

potentially enhance marine primary productivity (Schippers et al., 2004). For instance, across 18 stations in the central Atlantic Ocean primary productivity was stimulated by 15–19% under elevated dissolved CO_2 concentrations up to 36 μM (Hein and Sand-Jensen 1997). On the other hand, neutral effects of seawater acidification (SA) on growth rates of phytoplankton communities were reported in five of six CO_2 manipulation experiments in the coastal Pacific (Tortell et al., 2000). Furthermore, simulated future SA reduced surface PP in pelagic surface waters of Northern South China Sea and East China Sea (Gao et al., 2012). It seems that the impacts of SA on PP could be region-dependent. The varying effects of SA may be related to the regulation of other factors such as light intensity (Gao et al., 2012), temperature (Holding et al., 2015), nutrients (Tremblay et al., 2006) and community structure (Dutkiewicz et al., 2015).

Taiwan Strait of the East China Sea, located between southeast Mainland China and the Taiwan Island, is an important channel in transporting water and biogenic elements between the East China Sea and the South China Sea. Among the Chinese coastal areas, the Taiwan Strait is distinguished by its unique location. In addition to riverine inputs, it also receives nutrients from upwelling (Hong et al., 2011). Primary productivity is much higher in coastal waters than that in basin zones due to increased supply of nutrients through river runoff and upwelling (Chen, 2003; Cloern et al., 2014). The South China Sea, located from the equator to 23.8 °N, from 99.1 to 121.1 °E and encompassing an area of about 3.5×10^6 km^2, is one of the largest marginal seas in the world. As a marginal sea

of the Western Pacific Ocean, it has a deep semi-closed basin (with depths > 5000 m) and wide continental shelves, characterized by a tropical and subtropical climate (Jin et al., 2016). Approximately 80% of ocean organic carbon is buried in the Earth's continental shelves and therefore continental margins play an essential role in the ocean carbon cycle (Hedges & Keil, 1995). Investigating how SA affects primary productivity in the Taiwan Strait and the South China Sea could help us to understand the contribution of marginal seas to carbon sink under the future CO_2-increased scenarios. Although small-scale studies on SA impacts have been conducted in the East China Sea and the South China Sea (Gao et al., 2012, 2017), our understanding of how SA affects PP in marginal seas is still fragmentary and superficial. In this study, we conducted three cruises in the Taiwan Strait and the South China Sea, covering an area of 8.3×10^5 km^2, and aimed to provide in-depth insight into how SA and/or episodic pCO_2 rise affects PP in marginal seas with comparisons to other types of waters.

2 Materials and Methods

2.1 Investigation areas

To study the impacts of projected SA (dropping by ~0.4 pH) by the end of this century (RCP8.5) on marine primary productivity in different areas (Gattuso et al., 2015), we carried out deck-based experiments during the 3 cruises supported by National Natural Science Foundation of China (NSFC), which took place in the Taiwan Strait (Jul 14^{th}–25^{th}, 2016), the South China Sea basin (Sep 6–24^{th}, 2016), and the West South China

Sea (Sep 14th to Oct 24th, 2017), respectively. The experiments were conducted at 101 stations with coverage of 12 ^{o}N–26 ^{o}N and 110 ^{o}E–120 ^{o}E (Fig. 1). Investigation areas include the continental shelf (0–200 m, 22 stations) and the slope (200–3400 m, 44 stations), and the vast deep-water basin (> 3400 m, 35 stations). In the continental shelf, the areas with depth < 50 m are defined as coastal zones (9 stations).

2.2 Measurements of temperature and carbonate chemistry parameters

The temperature and salinity of surface seawater at each station were monitored with an onboard CTD (Seabird, USA). pH_{NBS} was measured with an Orion 2-Star pH meter (Thermo scientific, USA) that was calibrated with standard National Bureau of Standards (NBS) buffers (pH=4.01, 7.00, and 10.01 at 25.0 ^{o}C; Thermo Fisher Scientific Inc., USA). After the calibration, the electrode of pH meter was kept in surface seawater for half an hour and then the formal measurements were conducted. The analytical precision was ±0.001. Total alkalinity (TA) was determined using Gran titration on a 25-mL sample with a TA analyzer (AS-ALK1, Apollo SciTech, USA) that was regularly calibrated with certified reference materials supplied by A. G. Dickson at the Scripps Institution of Oceanography (Gao et al., 2018a). The analytical precision was ± 2 μmol kg^{-1}. CO_2 concentration in seawater and the pH_{Total} (pH_T) values was calculated by using CO2SYS (Pierrot et al., 2006) with the input of pH_{NBS} and TA data.

2.3 Solar radiation

The incident solar radiation intensity during the cruises was recorded with an

Eldonet broadband filter radiometer (Eldonet XP, Real Time Computer, Germany). This device has three channels for PAR (400–700 nm), UV-A (315–400 nm) and UV-B (280–315 nm) irradiance, respectively, which records the means of solar radiations over each minute. The instrument was fixed at the top layer of the ship to avoid shading.

2.4 Determination of primary productivity

Surface seawater (0–1m) was collected a 10 L acid-cleaned (1 M HCl) plastic bucket and pre-filtered (200 μm mesh size) to remove large grazers. To prepare high CO_2 (HC) seawater, CO_2-saturated seawater was added into pre-filtered seawater until a decrease of ~0.4 units in pH (corresponding CO_2 concentrations being 22.0–39.7 μM) was approached (Gattuso et al., 2010). Seawater that was collected from the same location as PP and filtered by cellulose acetate membrane (0.22 μm) was used to make the CO_2-saturated seawater, which was made by directly flushing with pure CO_2 until pH reached values around 4.50. When saturated-CO_2 seawater was added to the HC treatment, equivalent filtered seawater (without flushing with CO_2) was also added to the ambient CO_2 (AC) treatment as a control. The ratios of added saturated-CO_2 seawater to incubation seawater were about 1:1000. Samples were incubated within half an hour after they were collected. Prepared AC and HC seawater was allocated into 50-mL quartz tubes in triplicate, inoculated with 5 μCi (0.185 MBq) $NaH^{14}CO_3$ (ICN Radiochemicals, USA), and then incubated for 24 h (over a day-night cycle) under 100 % incident solar irradiances in a water bath for temperature control by running through surface seawater.

Due to heating by the deck, the temperatures in the water bath were 0–2 ^{o}C higher than in situ surface seawater temperatures. TA and pH of seawater before and after 24h incubation were measured to monitor the changes of carbonate systems. After the incubation, the cells were filtered onto GF/F filters (Whatman) and immediately frozen at −20 ℃ for later analysis. In the laboratory, the frozen filters were transferred to 20 mL scintillation vials, thawed and exposed to HCl fumes for 12 h, and dried (55 ℃, 6 h) to expel non-fixed ^{14}C, as previously reported (Gao et al., 2017). Then 3 mL scintillation cocktail (Perkin Elmer®, OptiPhase HiSafe) was added to each vial. After 2 h of reaction, the incorporated radioactivity was counted by a liquid scintillation counting (LS 6500, Beckman Coulter, USA). The carbon fixation for 24 h incubation was taken as chlorophyll (Chl) *a*-normalized daily primary productivity (PP, μg C (μg Chl *a*)$^{-1}$) (Gao et al., 2017). The changes (%) of PP induced by SA were expressed as (PP_{HC}−PP_{AC})/PP_{AC}×100, where PP_{HC} and PP_{AC} are the daily primary productivity under HC and AC, respectively.

2.5 Chl *a* measurement

Pre-filtered (200 μm mesh size) surface seawater (500–2000 mL) at each station was filtered onto GF/F filter (25 mm, Whatman) and then stored at -80 ^{o}C. After returning to laboratory, phytoplankton cells on the GF/F filter were extracted overnight in absolute methanol at 4 ^{o}C in darkness. After centrifugation (5000 *g* for 10 min), the absorption values of the supernatants were analyzed by a UV–VIS spectrophotometer (DU800,

154 Beckman, Fullerton, California, USA). The concentration of chlorophyll *a* (Chl *a*) was
155 calculated according to Porra (2002).

156 **2.6 Data analysis**

157 The data of environmental parameters were expressed in raw and the data of PP were
158 the means of triplicate incubations. Two-way analysis of variance (ANOVA) was used to
159 analyze the effects of SA and location on PP. Least significant difference (LSD) was used
160 to for *post hoc* analysis. Linear fitting analysis was conducted with Pearson correlation
161 analysis to assess the relationship between PP and environmental factors. A 95%
162 confidence level was used in all analyses.

163 **3 Results**

164 During the cruises, surface temperature ranged from 25.0 to 29.9 ^{o}C in the Taiwan
165 Strait and from 27.1 to 30.2 ^{o}C in the South China Sea (Fig. 2a). Surface salinity ranged
166 from 30.0 to 34.0 in the Taiwan Strait and from 31.0 to 34.3 in the South China Sea (Fig.
167 2b). The lower salinities were found in the estuaries of Minjiang and Jiulong Rivers as
168 well as Mekong River-induced Rip current. High salinities were found in the South China
169 Sea basin. Surface pH_T changed between 7.99–8.20 in the Taiwan Strait with the higher
170 values in the estuary of Minjiang River (Fig. 2c). Compared to the Taiwan Strait, the
171 South China Sea had lower surface pH (7.91–8.08) with the lowest value near the island
172 in the Philippines. TA ranged from 2100 to 2359 μmol kg^{-1} SW in the Taiwan Strait and
173 2126 to 2369 μmol kg^{-1} SW in the South China Sea (Fig. 2d). The lowest value occurred

in the estuary of Minjiang River. CO_2 concentration in surface seawater changed from 6.4–13.3 μmol kg^{-1} SW in the Taiwan Strait, and 9.3–14.3 μmol kg^{-1} SW in the South China Sea (Fig. 2e). It showed an opposite pattern to surface pH, with the lowest value in the estuary of Minjiang River in the Taiwan Strait and highest value in near the islands in the Philippines in the South China Sea. During the PP investigation period, the daytime mean PAR intensity ranged from 126.6 to 145.2 W m^{-2} s^{-1} in the Taiwan Strait and 37.3 to 150.0 W m^{-2} s^{-1} in the South China Sea (Fig. 2f).

The concentration of Chl *a* ranged from 0.11 to 12.13 μg L^{-1} in the Taiwan Strait (Fig. 3). The highest concentration occurred in the estuary of the Minjiang River. The concentration of Chl *a* in the South China Sea ranged from 0.037 to 7.43 μg L^{-1}. The highest concentration was found in the coastal areas of Guangdong province in China. For both the Taiwan Strait and the South China Sea, there were high Chl *a* concentrations (> 1.0 μg L^{-1}) in coastal areas, particularly in the estuaries of the Minjing River, Jiulong River and Pearl River. On the contrary, Chl *a* concentrations in offshore areas were lower than 0.2 μg L^{-1}.

Surface primary productivity changed from 99 to 302 μg C (μg Chl *a*)$^{-1}$ d^{-1} in the Taiwan Strait, and from 17 to 306 μg C (μg Chl *a*)$^{-1}$ d^{-1} in the South China Sea (Fig. 4). High surface primary productivity (> 200 μg C (μg Chl *a*)$^{-1}$ d^{-1}) was found in the estuaries of the Minjing River, Jiulong River, and Pearl River and areas near the East of Vietnam. In basin zones, the surface primary productivity was usually lower than 100 μg

194 C (μg Chl *a*)$^{-1}$ d^{-1}.

195 A series of onboard CO_2-enrich experiments in the investigated regions were
196 conducted during three cruises. In HC treatments, pH_{total} decreased by 0.34–0.43 units,
197 while pCO_2 and CO_2 increased by 676–982 μatm and 17–25 μmol kg^{-1} SW, respectively
198 (Table S1). Carbonate chemistry parameters after 24 h of incubation were stable (△pH <
199 0.06, △TA < 53 μmol kg^{-1} SW) , indicating the successful manipulation (Table S1). It
200 was observed that instantaneous effects of elevated pCO_2 on primary productivity of
201 surface phytoplankton community in all investigated regions ranged from -88%
202 (inhibition) to 57% (promotion), revealing significant regional differences among
203 continental shelf, slope and deep-water basin (ANOVA, $F_{(2, 98)} = 3.747$, $p = 0.027$, Fig. 5).
204 Among 101 stations, 70 stations showed insignificant SA effects. SA increased PP at 6
205 stations and reduced PP at 25 stations. Positive effects of SA on surface primary
206 productivity were observed in the Taiwan Strait and the western South China Sea (Fig. 5,
207 red-yellow shading areas), with the maximal enhancement of 57% in the station
208 approaching the Mekong River plume (LSD, $p < 0.001$). Reductions in PP induced by the
209 elevated CO_2 were mainly found in the central South China Sea basin within the latitudes
210 of 10 ^{o}N to 14 ^{o}N and the longitudes of 114.5 ^{o}E to 118 ^{o}E (Fig. 5, blue-purple shading
211 areas), with inhibition rates ranging from 24% to 88% (Fig. 5, LSD, $p < 0.05$). These
212 results showed a region-related effect of SA on photosynthetic carbon fixation of surface
213 phytoplankton assemblages. Overall, the elevated pCO_2 had neutral or positive effects on

primary productivity in the continental shelf and slope regions, while having adverse effects in the deep-water basin.

By analyzing the correlations between SA-induced PP changes and regional environmental parameters (Table S2), we found that SA-induced changes in phytoplankton primary productivity was significantly positively related with *in situ* pH ($p < 0.001$, $r = 0.379$), and PAR density ($p = 0.002$, $r = 0.311$) (Fig. 6). On the other hand, the influence induced by SA was negatively related to salinity that ranged from 30.00 to 34.28 ($p < 0.001$, $r = -0.418$).

4 Discussion

In the present study, we found that the elevated pCO_2 and associated pH drop increased or did not affect PP in the continental shelf and slope waters but reduced it in basin waters. Our results suggested that the enhanced effects of the SA treatment on photosynthetic carbon fixation depend on regions of different physicochemical conditions, including pH, light intensity and salinity. In addition, coastal diatoms appear to benefit more from SA than pelagic ones (Li et al., 2016). Therefore, community structure differences might also be responsible for the differences of the short-term high CO_2-induced acidification between coastal and basin waters.

SA is deemed to have two kinds of effects at least (Xu et al., 2017; Shi et al., 2019). The first one is the enrichment of CO_2, which is usually beneficial for photosynthetic carbon fixation and growth of algae because insufficient ambient CO_2 limits algal

234 photosynthesis (Hein & Sand-Jensen, 1997; Bach & Taucher, 2019). The other effect is
235 the decreased pH which could be harmful because it disturbs the acid-base balance
236 between extracellular and intracellular environments. For instance, the decreased pH
237 projected for future SA was shown to reduce the growth of the diazotroph *Trichodesmium*
238 (Hong et al., 2017), decrease PSII activity by reducing the removal rate of PsbD (D2)
239 (Gao et al., 2018b) and increase mitochondrial and photo-respirations in diatoms and
240 phytoplankton assemblages (Yang and Gao 2012, Jin et al., 2015). In addition, SA could
241 reduce the Rubisco transcription of diatoms, which also contributed to the decreased
242 growth (Endo et al., 2015). Therefore, the net impact of SA depends on the balance
243 between its positive and negative effects, leading to enhanced, inhibited or neutral
244 influences, as reported in diatoms (Gao et al., 2012, Li et al., 2021) and phytoplankton
245 assemblages in the Arctic and subarctic shelf seas (Hoppe et al., 2018), the North Sea
246 (Eberlein et al., 2017) and the South China Sea (Wu and Gao 2010, Gao et al., 2012). The
247 balance of positive and negative effects of SA can be regulated by other factors, including
248 pH, light intensity, salinity, population structure, etc. (Gao et al., 2019a, b; Xie et al.,
249 2022).

250 In the present study, SA increased or did not affect PP in coastal waters but reduced it
251 in offshore waters, which is significantly related to pH, light intensity and salinity (Fig. 6).
252 The effect of SA changed from negative to positive with the increase of local pH. The
253 higher pH occurred in coastal zones which may be caused by higher biomass of

phytoplankton (Fig. 3). Higher pH caused by intensive photosynthesis of phytoplankton is companied with decreased CO_2 levels. In this case, CO_2 is more limiting for photosynthesis of phytoplankton compared to lower pH. Therefore, SA could stimulate primary productivity via supplying more available CO_2 (Hurd et al., 2019). On the other hand, lower pH occurred in deep-water basin. Lower pH represents higher CO_2 availability. CO_2 is not limited or less limited in this case. Therefore, more CO_2 brought by SA may not benefit photosynthesis of phytoplankton. Instead, decreased pH accompanied by SA may inhibit photosynthesis or growth of phytoplankton, which is found in cyanobacteria (Hong et al., 2017). Furthermore, the negative effects of SA are particularly significant when nutrient is limited (Li et al., 2018). The nutrient levels in the basin are usually lower than on the shelf (Yuan et al., 2011; Lu et al., 2020; Du et al., 2021), which may exacerbate the negative effects of SA in the basin zone.

The negative effects of SA disappeared with increasing light intensity in this study. This results in inconsistent with Gao et al (2012)' study, in which SA increased photosynthetic carbon fixation of three diatoms (*Phaeodactylum tricornutum*, *Thalassiosira pseudonana* and *Skeletonema costatum*) under lower light intensities but decreased it under higher light intensities. The divergent findings may be due to different population structure that varies in different areas. Coastal zones where nutrients are relatively sufficient usually have abundant diatoms while picophytoplanktons mainly *Prochlorococcus* and *Synechococcus*, dominate oligotrophic areas (Xiao et al., 2018,

Zhong et al., 2020). In this study, most investigated areas are oligotrophic and thus the response of local phytoplankton to the combination of light intensity and SA may be different from diatoms. Meanwhile, the weak correlation (r = 0.311) between light intensity and SA effect suggests the deviation from linear relationship in the context of multiple variables needs to be further illuminated in future studies. It is worth noting that the samples were not mixed down in the water bath in the present study and exposed to 100% incident solar irradiances. Lower incident solar irradiances or some devices can be used to simulate seawater mixing in future studies. A negative correlation between SA-induced changes of PP and salinity was found in this study. The decrease of salinity (from 35 to 30) has been shown to alleviate the negative effect of SA on photosynthetic carbon fixation of a coccolithorphorid *Emiliania huxleyi* (Xu et al., 2020) although the potential mechanisms remain unknown. On the other hand, the change of salinity (from 6 to 3) did not affect effective quantum yield of microplanktonic community in the Baltic Sea grown under different CO_2 levels (Wulff et al., 2018). In this study, the negative relationship between salinity and SA effects seems to be an autocorrelation between salinity and in situ pH (Fig. S1) because lower salinity occurred in coastal waters where seawater pH was higher while the basin zone usually had higher salinities and lower pH.

The specific environmental conditions have profound effects on shaping diverse dominant phytoplankton groups (Boyd et al., 2010). Larger eukaryotic groups (especially diatoms) usually dominate the complex coastal regions, while picophytoplanktons

(*Prochlorococcus* and *Synechococcus*), characterizing with more efficient nutrients uptake, dominate the relatively stable offshore waters (Dutkiewicz et al., 2015). In summer and early autumn, previous investigations demonstrated that diatoms dominated in the northern waters and the Taiwan Strait (coastal and shelf regions) with high abundances of phytoplankton, which is consistent with our Chl *a* data; *Prochlorococcus* and *Synechococcus* dominated in the South China Sea basin and the north of South China Sea (slope and basin regions) (Xiao et al., 2018, Zhong et al., 2020). In addition, it has been reported that larger cells benefit more from SA because a thicker diffusion layer around the cells limits the transport of CO_2 (Feng et al., 2010; Wu et al., 2014). In contrast, a thinner diffusion layer and higher surface to volume ratio in smaller phytoplankton cells can make them easier to transport CO_2 near the cell surface and within the cells, and therefore picophytoplankton species are less CO_2-limited (Bao and Gao, 2021). Therefore, different community structures between coastal and basin areas could also be responsible for the enhanced and inhibitory effects of SA. It is worth noting that seasonality may also lead to the differential effects of SA on primary productivity since the Taiwan Strait cruise was conducted in July and the cruises of the South China Sea basin and the West South China Sea were conducted in September. The SST and solar PAR intensity of the Taiwan Strait in July was 2–3 ^{o}C and 22 $\pm$ 22 W m^{-2} s^{-1} higher than that in September (Zhang et al., 2008, 2009; Table S3). Although the effects of SA were not related to temperature as shown in this study (Table S2), the higher solar

radiation in July may contribute to the positive effect of SA on primary productivity. In addition, species succession of phytoplankton with season may also affect the response to SA (Xiao et al., 2018).

5 Conclusions

By investigating the impacts of the elevated pCO_2 on PP in the Taiwan Strait and the South China Sea, we demonstrated that such short SA-treatments induced changes in PP were mainly related to pH, light intensity and salinity based on Pearson correlation coefficients, supporting the hypothesis that negative impacts of SA on PP increase from coastal to basin waters (Gao et al., 2019a). In addition, phytoplankton community structures may also modulate SA induced changes. In view of ocean climate changes, strengthened stratification due to global warming would reduce the upward transports of nutrients and thus marine primary productivity. The negative effect of SA in basin zones may further reduce primary productivity. Meanwhile, PP in some coastal waters may be increased by SA.

Data availability. All data are included in the article or Supplement.

Author contributions. KG and TW developed the original idea and designed research. TW and JS carried out fieldwork. GG provided statistical analyses and prepared figures. GG, KG, and XZ wrote the manuscript. All contributed to revising the paper.

Competing interests. The contact author has declared that neither they nor their co-authors have any competing interests.

Disclaimer. Publisher's note: Copernicus Publications remains neutral with regard to jurisdictional claims in published maps and institutional affiliations.

Acknowledgements. This work was supported by the National Natural Science Foundation of China (41720104005, 41890803, 41721005, and 42076154) and the Fundamental Research Funds for the Central Universities (20720200111). The authors are grateful to the students He Li, Xiaowen Jiang and Shanying Tong, and the laboratory technicians Xianglan Zeng and Wenyan Zhao. We appreciate the NFSC Shiptime Sharing Project (project number: 41849901) for supporting the Taiwan Strait cruise (NORC2016-04). We appreciate the chief scientists Yihua Cai, Huabin Mao and Chen Shi and the R/V Yanping II, Shiyan I and Shiyan III for leading and conducting the cruises.

References

Bach, L. T., and Taucher, J.: CO_2 effects on diatoms: a synthesis of more than a decade of ocean acidification experiments with natural communities, Ocean Sci., 15, 1159-1175, 2019.

Bao, N., and Gao, K.: Interactive effects of elevated CO_2 concentration and light on the picophytoplankton *Synechococcus*, Front. Mar. Sci., 8, 1-7, 2021.

Boyd, P. W., Strzepek, R., Fu, F. X., and Hutchins, D. A.: Environmental control of open-ocean phytoplankton groups: Now and in the future, Limnol. Oceanogr, 55, 1353-1376, 2010.

Chen, C. T. A.: Rare northward flow in the Taiwan Strait in winter: A note, Cont. Shelf

354 Res., 23, 387-391, 2003.
355 Cloern, J. E., Foster, S.Q. and Kleckner, A. E.: Phytoplankton primary production in the
356 world's estuarine-coastal ecosystems, Biogeosciences, 11, 2477-2501, 2014.
357 Doney, S. C., Busch, D. S., Cooley, S. R., and Kroeker, K. J.: The impacts of ocean
358 acidification on marine ecosystems and reliant human communities, Annu. Rev. Env.
359 Resour., 45, 83-112, 2020.
360 Du, C., He, R., Liu, Z., Huang, T., Wang, L., Yuan, Z., Xu, Y., Wang, Z. and Dai, M.:
361 Climatology of nutrient distributions in the South China Sea based on a large data
362 set derived from a new algorithm. Prog. Oceanogr., 195, 102586, 2021.
363 Dutkiewicz, S., Morris, J. J., Follows, M. J., Scott, J., Levitan, O., Dyhrman, S. T., and
364 Berman-Frank, I.: Impact of ocean acidification on the structure of future
365 phytoplankton communities, Nat. Clim. Change, 5, 1002-1006, 2015.
366 Eberlein, T., Wohlrab, S., Rost, B., John, U., Bach, L. T., Riebesell, U., and Van de Waal,
367 D. B.: Effects of ocean acidification on primary production in a coastal North Sea
368 phytoplankton community, Plos One, 12, 1-15, 2017.
369 Endo, H., Sugie, K., Yoshimura, T., and Suzuki, K.: Effects of CO_2 and iron availability
370 on rbcL gene expression in Bering Sea diatoms, Biogeosciences, 12, 2247-2259,
371 2015.
372 Feng, Y., Hare, C. E., Rose, J. M., Handy, S. M., DiTullio, G. R., Lee, P. A., Smith, W. O.,
373 Peloquin, J., Tozzi, S., Sun, J., Zhang, Y., Dunbar, R. B., Long, M. C., Sohst, B.,

Lohan, M., and Hutchins, D. A.: Interactive effects of iron, irradiance and CO_2 on Ross Sea phytoplankton, Deep-Sea Res. PT. I, 57, 368-383, 2010.

Gao, G., Xu, Z. G., Shi, Q., and Wu, H. Y.: Increased CO_2 exacerbates the stress of ultraviolet radiation on photosystem II function in the diatom *Thalassiosira weissflogii*, Environ. Exp. Bot., 156, 96-105, 2018b.

Gao, G., Jin, P., Liu, N., Li, F. T., Tong, S. Y., Hutchins, D. A., and Gao, K. S.: The acclimation process of phytoplankton biomass, carbon fixation and respiration to the combined effects of elevated temperature and pCO_2 in the northern South China Sea, Mar. Pollut. Bull., 118, 213-220, 2017.

Gao, G., Qu, L., Xu, T., Burgess, J.G., Li, X. and Xu, J.: Future CO_2-induced ocean acidification enhances resilience of a green tide alga to low-salinity stress. ICES J. Mar. Sci., 76, 2437-2445, 2019b.

Gao, G., Xia, J. R., Yu, J. L., Fan, J. L., and Zeng, X. P.: Regulation of inorganic carbon acquisition in a red tide alga (*Skeletonema costatum*): The importance of phosphorus availability, Biogeosciences, 15, 4871-4882, 2018a.

Gao, K. S., Beardall, J., Häder, D. P., Hall-Spencer, J. M., Gao, G., and Hutchins, D. A.: Effects of ocean acidification on marine photosynthetic organisms under the concurrent influences of warming, UV radiation, and deoxygenation, Front. Mar. Sci., 6, 1-18, 2019a.

Gao, K. S., Xu, J. T., Gao, G., Li, Y. H., Hutchins, D. A., Huang, B. Q., Wang, L., Zheng,

394 Y., Jin, P., Cai, X. N., Hader, D. P., Li, W., Xu, K., Liu, N. N., and Riebesell, U.:
395 Rising CO_2 and increased light exposure synergistically reduce marine primary
396 productivity, Nat. Clim. Change, 2, 519-523, 2012.
397 Gattuso, J. P., Gao, K. S., Lee, K., Rost, B., and Schulz, K. G.: Approaches and tools to
398 manipulate the carbonate chemistry, pp 41-52. Guide to best practices for ocean
399 acidification research and data reporting, edited by: Riebesell, U., Fabry, V. J.,
400 Hansson, L., and Gattuso J.-P., Luxembourg: Publications Office of the European
401 Union, 2010.
402 Gattuso, J. P., Magnan, A., Billé, R., Cheung, W. W. L., Howes, E. L., Joos, F., Allemand,
403 D., Bopp, L., Cooley, S. R., Eakin, C. M., Hoegh-Guldberg, O., Kelly, R. P., Portner,
404 H. O., Rogers, A. D., Baxter, J. M., Laffoley, D., Osborn, D., Rankovic, A., Rochette,
405 J., Sumaila, U. R., Treyer, S., and Turley, C.: Contrasting futures for ocean and
406 society from different anthropogenic CO_2 emissions scenarios, Science, 349,
407 aac4722, 2015.
408 Hedges, J. I., and Keil, R. G.: Sedimentary organic matter preservation: an assessment
409 and speculative synthesis, Mar. Chem., 49, 81-115, 1995.
410 Hein, M., and Sand-Jensen, K.: CO_2 increases oceanic primary production, Nature, 388,
411 526-527, 1997.
412 Hennon, G. M. M., Ashworth, J., Groussman, R. D., Berthiaume, C., Morales, R. L.,
413 Baliga, N. S., Orellana, M. V., and Armbrust, E. V.: Diatom acclimation to elevated

CO_2 via cAMP signalling and coordinated gene expression, Nat. Clim. Change, 5, 761-765, 2015.

Holding, J. M., Duarte, C. M., Sanz-Mart ń, M., Mesa, E., Arrieta, J. M., Chierici, M., Hendriks, I. E., Garcia-Corral, L. S., Regaudie-de-Gioux, A., Delgado, A., Reigstad, M., Wassmann, P., and Agusti, S.: Temperature dependence of CO_2-enhanced primary production in the European Arctic Ocean, Nat. Clim. Change, 5, 1079-1082, 2015.

Hong, H. S., Chai, F., Zhang, C. Y., Huang, B. Q., Jiang, Y. W., and Hu, J. Y.: An overview of physical and biogeochemical processes and ecosystem dynamics in the Taiwan Strait, Cont. Shelf Res., 31, S3-S12, 2011.

Hong, H. Z., Shen, R., Zhang, F. T., Wen, Z. Z., Chang, S. W., Lin, W. F., Kranz, S. A., Luo, Y. W., Kao, S. J., Morel, F. M. M. and Shi, D. L.: The complex effects of ocean acidification on the prominent N_2-fixing cyanobacterium *Trichodesmium*. Science, 356, 527-530, 2017.

Hopkinson, B. M., Dupont, C. L., Allen, A. E., and Morel, F. M.: Efficiency of the CO_2-concentrating mechanism of diatoms, P. Natl. Acad. Sci. USA., 108, 3830-3837, 2011.

Hoppe, C. J. M., Wolf, K. K. E., Schuback, N., Tortell, P. D., and Rost, B.: Compensation of ocean acidification effects in Arctic phytoplankton assemblages. Nat. Clim. Change, 8, 529-533, 2018.

Hurd, C.L., Beardall, J., Comeau, S., Cornwall, C.E., Havenhand, J.N., Munday, P.L., Parker, L.M., Raven, J.A. and McGraw, C.M.: Ocean acidification as a multiple driver: how interactions between changing seawater carbonate parameters affect marine life. Mari. Freshwater Res., 71, 263-274, 2019.

IPCC, 2019: IPCC Special Report on the Ocean and Cryosphere in a Changing Climate [H.-O. Pörtner, D.C. Roberts, V. Masson-Delmotte, P. Zhai, M. Tignor, E. Poloczanska, K. Mintenbeck, A. Alegría, M. Nicolai, A. Okem, J. Petzold, B. Rama, N.M. Weyer (eds.)]. In press.

Jin, P., Gao, G., Liu, X., Li, F. T., Tong, S. Y., Ding, J. C., Zhong, Z. H., Liu, N. N., and Gao, K. S.: Contrasting photophysiological characteristics of phytoplankton assemblages in the Northern South China Sea, Plos One, 11, 1-16, 2016.

Jin, P., Wang, T. F., Liu, N. N., Dupont, S., Beardall, J., Boyd, P. W., Riebesell, U., and Gao, K. S.: Ocean acidification increases the accumulation of toxic phenolic compounds across trophic levels, Nat. Commun., 6, 1-6, 2015.

Li, F. T., Wu, Y. P., Hutchins, D. A., Fu, F. X., and Gao, K. S.: Physiological responses of coastal and oceanic diatoms to diurnal fluctuations in seawater carbonate chemistry under two CO_2 concentrations, Biogeosciences, 13, 6247-6259, 2016.

Li, F. T., Beardall, J., and Gao, K. S.: Diatom performance in a future ocean: interactions between nitrogen limitation, temperature, and CO_2-induced seawater acidification, ICES J. Mar. Sci., 75, 1451-1464, 2018.

Li, H. X., Xu, T. P., Ma, J., Li, F. T., and Xu, J. T.: Physiological responses of *Skeletonema costatum* to the interactions of seawater acidification and the combination of photoperiod and temperature, Biogeosciences, 18, 1439-1449, 2021.

Lu, Z., Gan, J., Dai, M., Zhao, X. and Hui, C. R.: Nutrient transport and dynamics in the South China Sea: A modeling study. Prog. Oceanogr., 183, 102308, 2020.

Moreau, S., Penna, A. D., Llort, J., Patel, R., Langlais, C., Boyd, P. W., Matear, R. J., Phillips, H. E., Trull, T. W., Tilbrook, B. and Lenton, A.: Eddy-induced carbon transport across the Antarctic Circumpolar Current. Global Biogeochem. Cy., 31, 1368-1386, 2017

Mostofa, K.M., Liu, C.Q., Zhai, W., Minella, M., Vione, D., Gao, K., Minakata, D., Arakaki, T., Yoshioka, T., Hayakawa, K. and Konohira, E.: Reviews and Syntheses: Ocean acidification and its potential impacts on marine ecosystems, Biogeosciences, 13, 1767-1786, 2016.

Pierrot, D., Wallace, D.W. R., and Lewis, E.: MS Excel program developed for CO_2 system calculations. ORNL/CDIAC-105a, Carbon Dioxide Information Analysis Center, Oak Ridge National Laboratory, US Department of Energy, Oak Ridge, Tennessee, USA., 2006.

Porra, R. J.: The chequered history of the development and use of simultaneous equations for the accurate determination of chlorophylls a and b, Photosynth. Res., 73, 149-156, 2002.

Raven, J. A., and Beardall, J.: CO_2 concentrating mechanisms and environmental change, Aquat. Bot., 118, 24-37, 2014.

Schippers, P., Lürling, M., and Scheffer, M.: Increase of atmospheric CO_2 promotes phytoplankton productivity, Ecol. Lett., 7, 446-451, 2004.

Shi, D. L., Hong, H. Z., Su, X., Liao, L. R., Chang, S. W., and Lin, W. F.: The physiological response of marine diatoms to ocean acidification: Differential roles of seawater pCO_2 and pH, J. Phycol., 55, 521-533, 2019.

Tortell, P. D., Rau, G. H., and Morel, F. M. M.: Inorganic carbon acquisition in coastal Pacific phytoplankton communities, Limnol. Oceanogr., 45, 1485-1500, 2000.

Tremblay, J. E., Michel, C., Hobson, K. A., Gosselin, M., and Price, N. M.: Bloom dynamics in early opening waters of the Arctic Ocean. Limnol. Oceanogr., 51, 900-912, 2006.

Riebesell, U., Aberle-Malzahn, N., Achterberg, E. P., Algueró-Muñiz, M., Alvarez-Fernandez, S., Arístegui, J., Bach, L. T., Boersma, M., Boxhammer, T., Guan, W. C., Haunost, M., Horn, H. G., Loscher, C. R., Ludwig, A., Spisla, C., Sswat, M., Stange, P., and Taucher, J.: Toxic algal bloom induced by ocean acidification disrupts the pelagic food web, Nat. Clim. Change, 8, 1082-1086, 2018.

Wu, Y., Gao, K., and Riebesell, U.: CO_2-induced seawater acidification affects physiological performance of the marine diatom *Phaeodactylum tricornutum*, Biogeosciences, 7, 2915-2923, 2010.

Wu, Y., Campbell, D. A., Irwin, A. J., Suggett, D. J., and Finkel, Z. V.: Ocean acidification enhances the growth rate of larger diatoms. Limnol. Oceanogr., 59, 1027-1034, 2014.

Wulff, A., Karlberg, M., Olofsson, M., Torstensson, A., Riemann, L., Steinhoff, F. S., Mohlin, M., Ekstrand, N., and Chierici, M.: Ocean acidification and desalination: Climate-driven change in a Baltic Sea summer microplanktonic community, Mar. Biol., 165, 1-15, 2018.

Xiao, W. P., Wang, L., Laws, E., Xie, Y. Y., Chen, J. X., Liu, X., Chen, B. Z., and Huang, B. Q.: Realized niches explain spatial gradients in seasonal abundance of phytoplankton groups in the South China Sea, Prog. Oceanogr., 162, 223-239, 2018.

Xie, S., Lin, F., Zhao, X. and Gao, G.: Enhanced lipid productivity coupled with carbon and nitrogen removal of the diatom *Skeletonema costatum* cultured in the high CO_2 level. Algal Res. 61, 102589, 2022.

Xu, J. K., Sun, J. Z., Beardall, J., and Gao, K. S.: Lower salinity leads to improved physiological performance in the coccolithophorid *Emiliania huxleyi*, which partly ameliorates the effects of ocean acidification, Front. Mar. Sci., 7, 1-18, 2020.

Xu, Z. G., Gao, G., Xu, J. T., and Wu, H. Y.: Physiological response of a golden tide alga (*Sargassum muticum*) to the interaction of ocean acidification and phosphorus enrichment, Biogeosciences, 14, 671-681, 2017.

Yang, G. Y., and Gao, K. S.: Physiological responses of the marine diatom *Thalassiosira*

514 *pseudonana* to increased pCO_2 and seawater acidity, Mar. Environ. Res., 79,
515 142-151, 2012.
516 Yu, P., Wang, Z. A., Churchill, J., Zheng, M., Pan, J., Bai, Y., and Liang, C.: Effects of
517 typhoons on surface seawater pCO_2 and air-sea CO_2 fluxes in the northern South
518 China Sea. J. Geophys. Res-Oceans, 125, p.e2020JC016258, 2020.
519 Yuan, X., He, L., Yin, K., Pan, G., and Harrison, P. J.: Bacterial distribution and nutrient
520 limitation in relation to different water masses in the coastal and northwestern South
521 China Sea in late summer. Cont. Shelf Res., 31, 1214-1223, 2011.
522 Zhang, C., Zhang, X., Zeng, Y., Pan, W., Lin J.: Retrieval and validation of sea surface
523 temperature in the Taiwan Strait using MODIS data. Acta Oceanol. Sin., 30, 153-160,
524 2008.
525 Zhang, C., Ren, Y., Cai, Y., Zeng, Y., and Zhang, X.: Study on local monitoring model for
526 SST in Taiwan strait based on MODIS data. J. Trop. Meteorol., 25, 73-81, 2009.
527 Zhong, Y. P., Liu, X., Xiao, W. P., Laws, E. A., Chen, J. X., Wang, L., Liu, S. G., Zhang,
528 F., and Huang, B. Q.: Phytoplankton community patterns in the Taiwan Strait match
529 the characteristics of their realized niches, Prog. Oceanogr., 186, 1-15, 2020.

Figure captions

Fig. 1 Sampling stations for the incubation experiments in the Taiwan Strait and the South China Sea during three cruises. Taiwan Strait cruise was conducted in July 2016 (red dots), South China Sea Basin cruise were conducted in September 2016 (blue dots) and Western South China Sea cruise was conducted in September 2017 (black dots).

Fig. 2 Temperature (^{o}C, panel a), salinity (panel b), pH_{total} (panel c), total alkalinity (μmol kg^{-1} SW, panel d), and CO_2 (μmol kg^{-1} SW, panel e) in surface seawater and mean PAR intensity (W m^{-2} s^{-1}, panel f) during the PP incubation experiments.

Fig. 3 Chl *a* concentration (μg L^{-1}) in the Taiwan Strait and the South China Sea during research cruises.

Fig. 4 Surface primary productivity (μg C (μg Chl *a*)$^{-1}$ d^{-1}) in the Taiwan Strait and the South China Sea during research cruises.

Fig. 5 Seawater acidification (pH decreases of 0.4 units) induced changes (%) of surface primary productivity in the Taiwan Strait and the South China Sea. Red-yellow shading represents a positive effect on PP and blue-purple shading represents a negative effect.

Fig. 6 Seawater acidification (pH decreases of 0.4 units) induced changes on surface primary productivity (%) in the South China Sea as a function of ambient pH_{total} (a), PAR (b), and salinity (c). The dotted lines represent 95% confidence intervals.

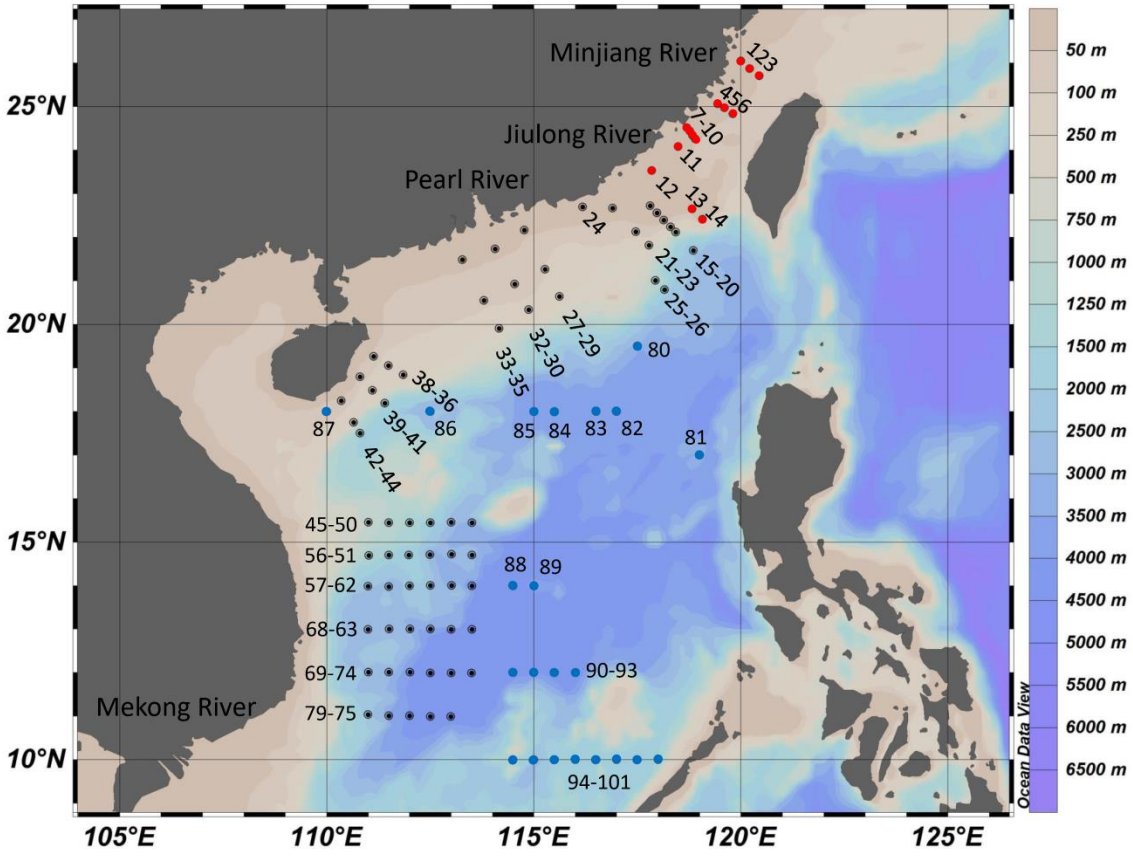
Minjiang River
Jiulong River
Pearl River
Mekong River
123
456
7-10
11
12
13
14
24
15-20
21-23
25-26
27-29
32-30
33-35
38-36
39-41
42-44
87
86
85
84
83
82
81
80
45-50
56-51
57-62
68-63
69-74
79-75
88
89
90-93
94-101
25°N
20°N
15°N
10°N
105°E
110°E
115°E
120°E
125°E
50 m
100 m
250 m
500 m
750 m
1000 m
1250 m
1500 m
2000 m
2500 m
3000 m
3500 m
4000 m
4500 m
5000 m
5500 m
6000 m
6500 m
Ocean Data View

Fig. 1

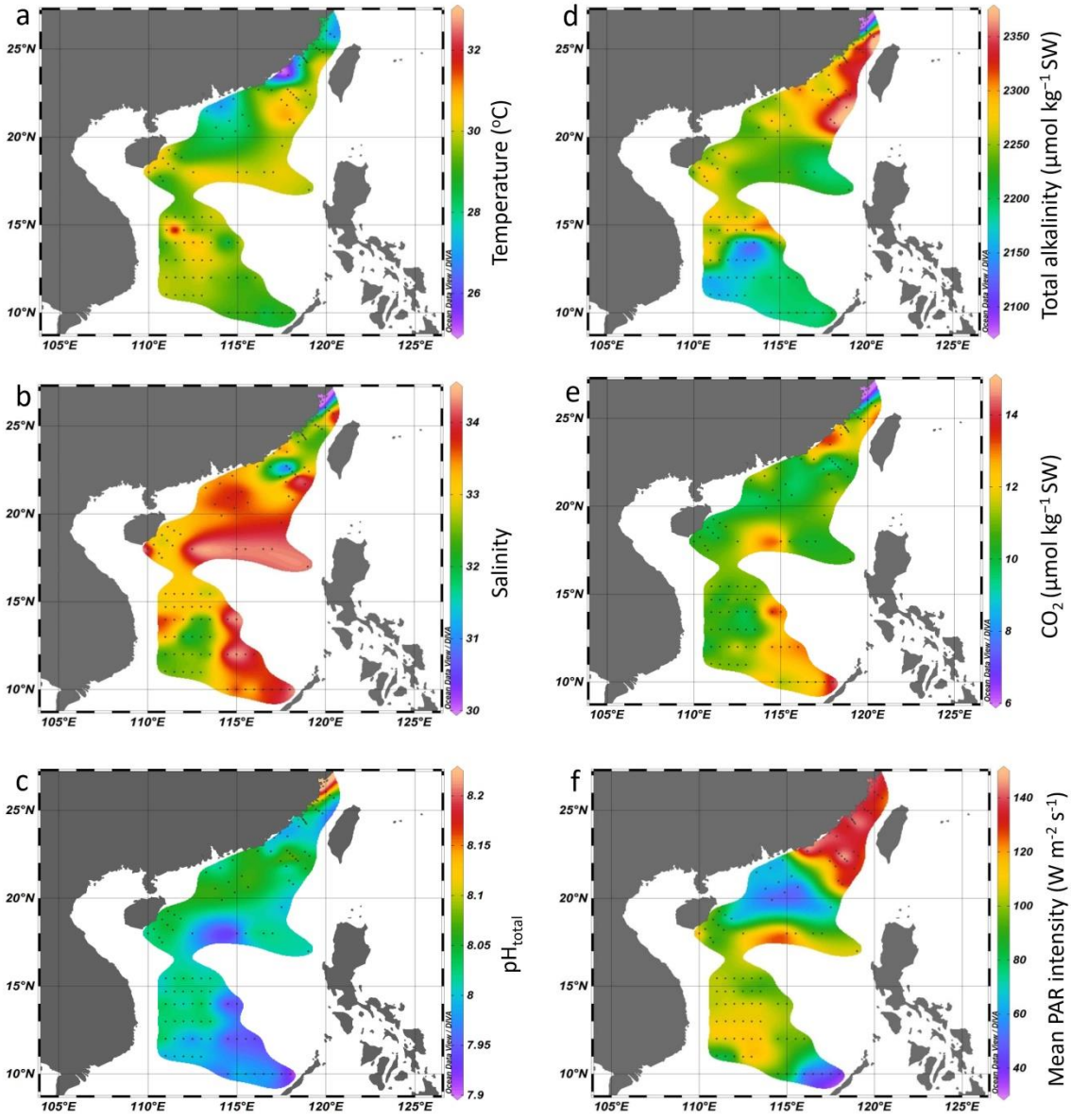
a
b
c
d
e
f
25°N
20°N
15°N
10°N
105°E
110°E
115°E
120°E
125°E
Temperature (°C)
32
30
28
26
Salinity
34
33
32
31
30
pH$_{total}$
8.2
8.15
8.1
8.05
8
7.95
7.9
Total alkalinity (µmol kg^{-1} SW)
2350
2300
2250
2200
2150
2100
CO_2 (µmol kg^{-1} SW)
14
12
10
8
6
Mean PAR intensity (W m^{-2} s^{-1})
140
120
100
80
60
40
Ocean Data View / DIVA

Fig. 2

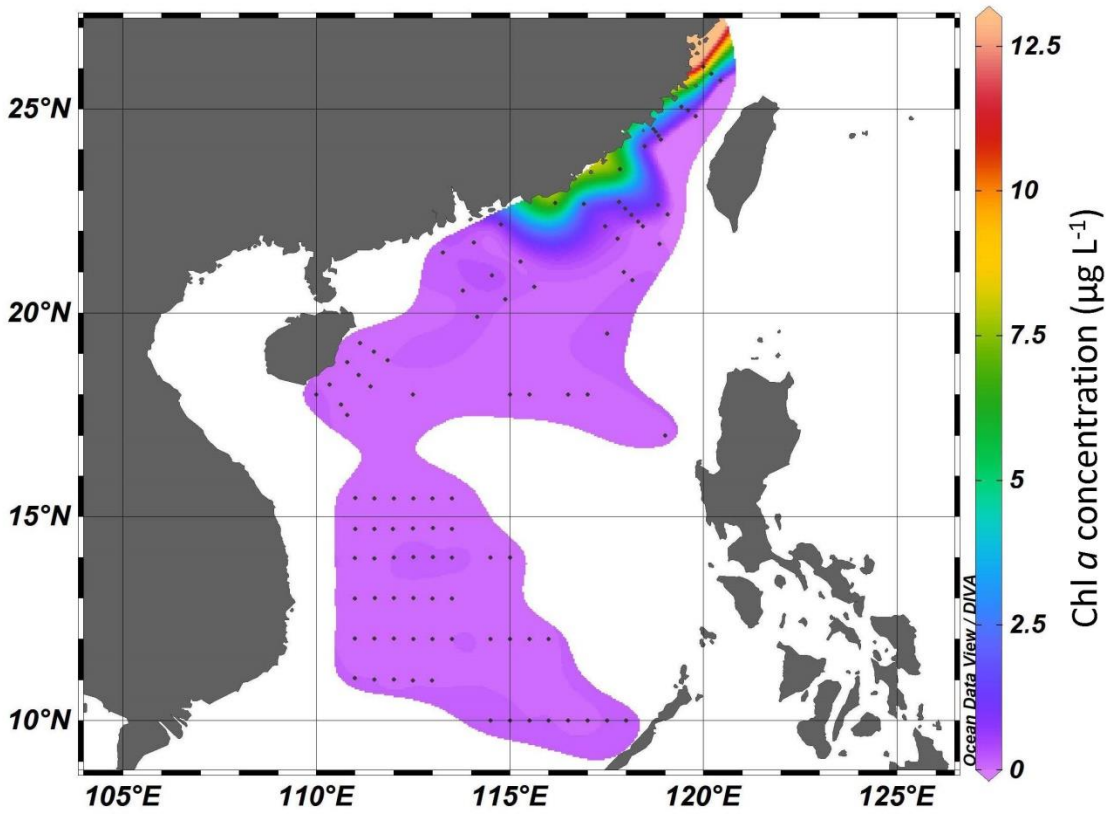
25°N
20°N
15°N
10°N
105°E
110°E
115°E
120°E
125°E
12.5
10
7.5
5
2.5
0
Chl a concentration (µg L-1)
Ocean Data View / DIVA

Fig. 3

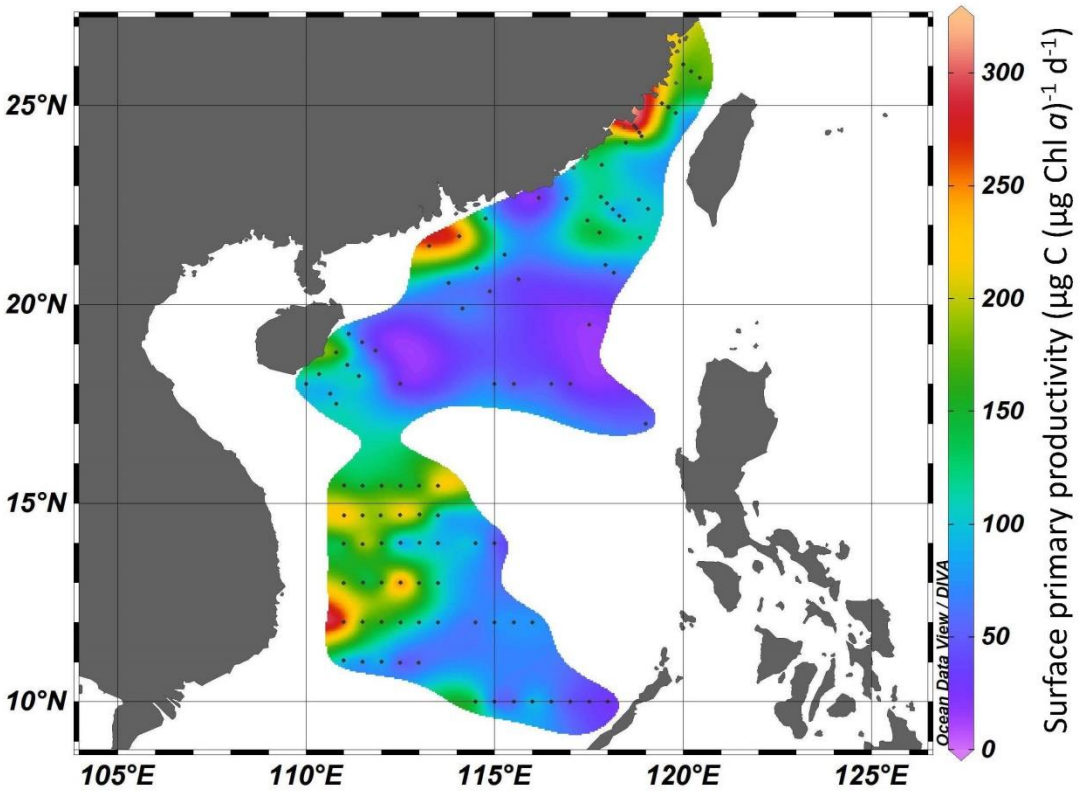
25°N
20°N
15°N
10°N
105°E
110°E
115°E
120°E
125°E
300
250
200
150
100
50
0
Surface primary productivity (µg C (µg Chl a)-1 d-1)
Ocean Data View / DIVA

Fig. 4

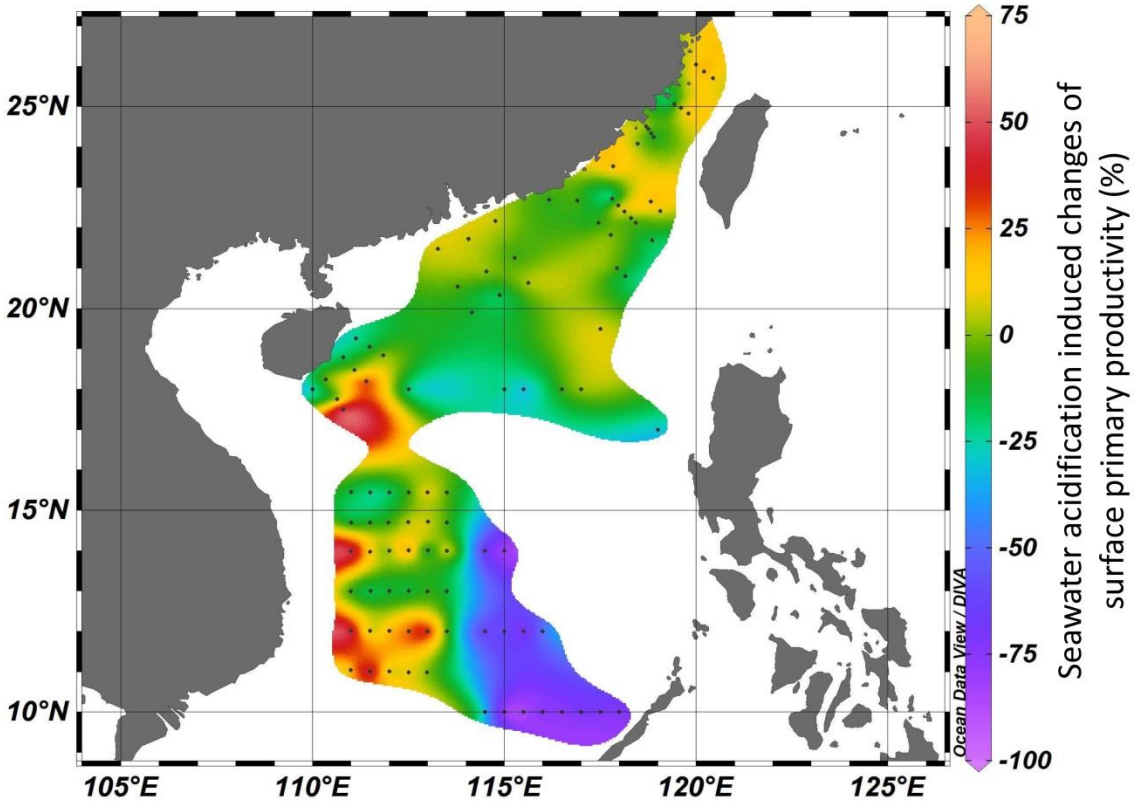
25°N
20°N
15°N
10°N
105°E
110°E
115°E
120°E
125°E
75
50
25
0
-25
-50
-75
-100
Seawater acidification induced changes of surface primary productivity (%)
Ocean Data View / DIVA

Fig. 5

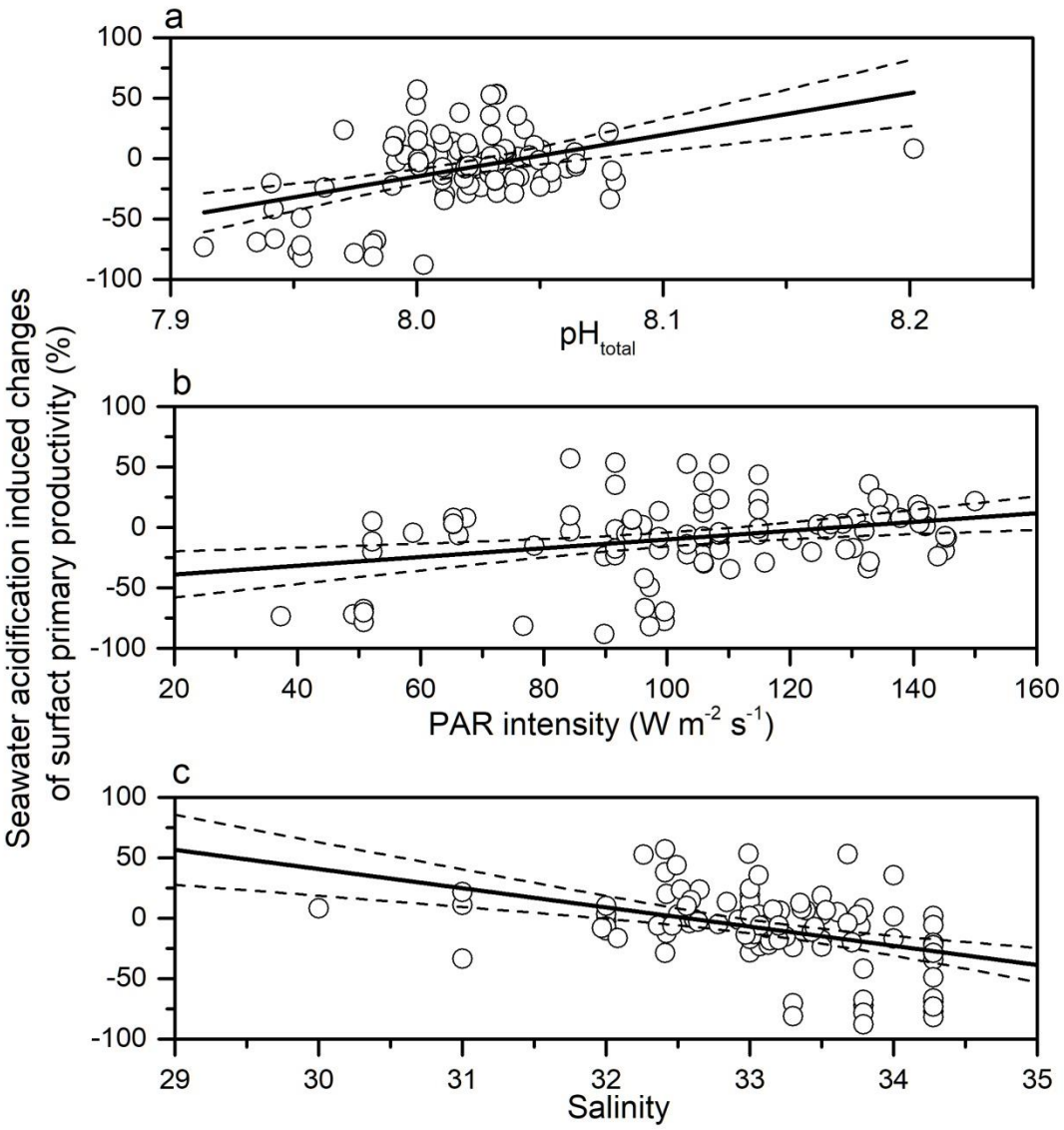
a
b
c
Seawater acidification induced changes of surfact primary productivity (%)
pH$_{total}$
PAR intensity (W m^{-2} s^{-1})
Salinity
100
50
0
-50
-100
7.9
8.0
8.1
8.2
20
40
60
80
100
120
140
160
29
30
31
32
33
34
35

Fig. 6